Scientific Research Publishing

Computational Chemistry, 2022, 10, 139-156
https://www.scirp.org/journal/cc
ISSN Online: 2332-5984
ISSN Print: 2332-5968

Mechanism of Degradation of Rice Starch Amylopectin by Oryzenin Using ONIOM Quantum Calculations [DFT/B3LYP/6-31+G(D, P): AM1]

Bamba El Hadji Sawaliho*, N'Guessan Boka Robert

Laboratoire de Constitution et de Réaction de la Matière, UFR SSMT, Université Félix Houphouët-Boigny, Abidjan, Côte d'Ivoire
Email: *bambaelhadjisawaliho@yahoo.ca

How to cite this paper: El Hadji Sawaliho, B. and Robert, N.B. (2022) Mechanism of Degradation of Rice Starch Amylopectin by Oryzenin Using ONIOM Quantum Calculations [DFT/B3LYP/6-31+G(D, P): AM1]. *Computational Chemistry*, **10**, 139-156.
https://doi.org/10.4236/cc.2022.104007

Received: June 9, 2022
Accepted: August 28, 2022
Published: August 31, 2022

Abstract

Understanding the molecular factors of rice degradation during its aging concerns our research team. This article emphasizes oryzenin-amylopectin. It aims to reveal the mechanism of amylopectin deterioration during rice aging. The research exploits the Natural Bond Analysis and ONION method at theory level DFT/B3LYP/6-31+G(d, p) and AM1. This methodological approach allows highlighting amylopectin transformation; oryzenin converts amylopectin into amyloidosis in continuous. This led to monosaccharides and disaccharides.

Keywords

Amylopectin, Hydrogen Bond, Theoretical Method, Starch, Oryzenin

1. Introduction

Rice is the staple food of the Ivorian people. However, Côte d'Ivoire is struggling to fulfill food self-sufficiency in relation to this product. Post-harvest losses are the main cause. They're explained by the inefficiency of storage techniques or its alteration during storage. Understanding the molecular factors of this modification concerns our research team. This work follows up on two others on the subject. The first focuses on the roles of phospholipids in this process [1]. The second analyzes the oryzenin-amyloidosis interaction [2]. This article emphasizes oryzenin-amylopectin. It aims to elucidate the role of this latter in the degradation of rice.

Previous work on amyloidosis establishes that its degradation occurs due to its

transformation into polysaccharides and monosaccharides [2]. On the contrary, authors [3] explain its alteration by the slow transformation of amylose into amylopectin. They conjecture that this transformation results in a compensatory increase in the second. This debate suggests the following research question:

How does oryzenin interact with amylopectin?

This work aims to understand the mechanism that degrades the components of starch; literature ignores it. Moreover, theoretical studies on amylopectin-oryzenin remain unknown. The research targets to contribute to filling this gap. It assumes that the hydrogen bond (HB) between oryzenin and amylopectin decomposes this latter; its formation impacts the stability of many molecules in the solid state and in solution. It justifies those of molecular structures such as DNA, water [4] [5] and carboxylic acids [6] [7].

HB influences some physical constants such as the melting point temperature of chemical compounds. To answer the research question, this work utilizes the resources of theoretical chemistry. It deploys NBO (Natural Bond Orbital) analysis [8]; it uses charge transfer (CT) [9] [10] [11] to describe the formation of HB as in [2]. Additionally, it exploits the branching model to guide calculations of oryzenin-amylopectin interactions. It relies on an amylopectin subunit; this contains three (AMP3G) or four (AMP4G) glucose molecules linked by sugar bridges. Also, the research employs the resources of quantum chemistry.

This work applies the ONION method at precision [DFT/B3LYP/6-31+G(d, p): AM1] and AM1. Furthermore, amylopectin molecules schematize with three (AMP3G) and four (AMP4G) molecules of α-D glucose or synthons connected by osidic bridges. This methodology highlights the mechanism shaping the degradation of amylopectin under the action of oryzenin. This knowledge, associated with that of the amyloidosis degradation, helps to clarify the mechanism underlying the degradation of rice starch during its prolonged storage. This article consists of three parts.

The first details the results of the Natural Bond Orbital (NBO) analysis. The second focuses on the AMP3G-oryzenin interaction. The third examines the one between the latter and AMP4G. These last two parts present the geometrical, energetic, and spectroscopic parameters of these complexes. Also, it discusses the convergent or divergent aspects between the results obtained with amyloidosis. Before, the article summarizes the hardware and the materials and the method of research.

2. Materials and Method of Research

This work retains the strategy used to study the amylose-oryzenin interaction. The amylopectin subunits comprise three (AMP3G) or four (AMP4G) glucose molecules linked by osidic bridges. The arrangement of glucose molecules considers the branching of amylopectin. The amylopectin-oryzenin complex is divided into two parts. The ONIOM/[DFT/B3LYP/6-31+G(d, p): AM1] offers the possibility of calculating its parameters with different levels of precision [12]

[13]. The active part concerns the interaction site between the hydrogen of oryzenin and the oxygen of amylopectin. This part undergoes a calculation with high precision DFT/(B3LYP/6-31+G(d, p)). On the contrary, the remaining part of the complex is treated with the low precision semi-empirical AM1 method. Moreover, the research uses Gaussian 09 software to optimize all the parameters of the complexes [14].

Vibration frequency calculations help validate their geometric parameters. From an ideal structure, a "single point" calculation at the same level of theory offers the opportunity to perform the NBO calculation [15]. As in the amylose-oryzenin complexes, the interactions considered are those established between osidic oxygen of amylopectin (by its subunits) and oryzenin-hydrogen. The numbering of the atoms is generated automatically by the GaussView06 software. The electrostatic potential [16] [17] [18] [19] at the level of the B3LYP/6-31+G(d, p) theory makes it possible to identify the HB donor or acceptor sites of oryzenin [2]. More, this article presents and discusses its results.

3. Results and Discussion

This section presents the results related to the interactions between the two polysaccharides of the study and oryzenin. It specifies those linking to the NBO analysis. Table 1 and Table 2 present the stabilization energies $E^{(2)}$, the differences

Table 1. Stabilization energy of second-order $E^{(2)}$ perturbations in the AMP3G-oryzenin complex.

Interactions	Transitions	$E^{(2)}$ Kcal/mol	E(i) - E(j) (a.u)	F(i, j) (a.u)	CT (me)
oryzenin-H_{30}…O_{49}	$n^{(1)}_{Cl_{36}} \rightarrow \sigma^{*}_{O_{69}\text{-}H_{77}}$	3.08	0.9	0.049	5.93
	$n^{(2)}_{Cl_{36}} \rightarrow \sigma^{*}_{O_{69}\text{-}H_{77}}$	2.17	0.8	0.039	4.75
	$n^{(4)}_{Cl_{36}} \rightarrow \sigma^{*}_{C_{69}\text{-}H_{77}}$	51.82	0.71	0.172	117.37
	$n^{(1)}_{O_{49}} \rightarrow \sigma^{*}_{O_{29}\text{-}H_{30}}$	3.74	1.02	0.055	5.82
	$n^{(2)}_{O_{49}} \rightarrow \sigma^{*}_{O_{29}\text{-}H_{30}}$	8.46	0.82	0.075	16.73
	$n^{(1)}_{O_{69}} \rightarrow \sigma^{*}_{C_{26}\text{-}H_{28}}$	3.94	1.01	0.056	6.15
	$n^{(1)}_{O_{69}} \rightarrow \sigma^{*}_{C_{26}\text{-}H_{28}}$	1.24	0.73	0.027	2.74
oryzenin-H_{30}…O_{99}	$n^{(2)}_{Cl_{36}} \rightarrow \sigma^{*}_{O_{91}\text{-}H_{102}}$	2.43	1.01	0.045	3.97
	$n^{(4)}_{Cl_{36}} \rightarrow \sigma^{*}_{O_{91}\text{-}H_{102}}$	38.5	0.81	0.158	76.10
	$n^{(1)}_{O_{91}} \rightarrow \sigma^{*}_{C_{26}\text{-}H_{28}}$	4.04	1.00	0.057	6.50
	$n^{(1)}_{O_{99}} \rightarrow \sigma^{*}_{C_{29}\text{-}H_{30}}$	2.44	1.02	0.045	3.89
	$n^{(2)}_{O_{99}} \rightarrow \sigma^{*}_{C_{29}\text{-}H_{30}}$	10.59	0.83	0.085	20.98
N_9-H_{10}…O_{49}	$n^{(2)}_{O_{37}} \rightarrow \sigma^{*}_{C_{11}\text{-}H_{13}}$	1.85	0.76	0.034	4.00
	$n^{(1)}_{O_{49}} \rightarrow \sigma^{*}_{N_9\text{-}H_{10}}$	5.96	1.03	0.07	9.24
N_9-H_{10}…O_{99}	$n^{(1)}_{O_{99}} \rightarrow \sigma^{*}_{N_9\text{-}H_{10}}$	4.32	0.98	0.058	7.00
	$n^{(2)}_{O_{99}} \rightarrow \sigma^{*}_{N_9\text{-}H_{10}}$	8.59	0.79	0.074	17.55

Table 2. Stabilization energy of second-order $E^{(2)}$ perturbations in the AMP4G-oryzenin complex.

Interactions	Transitions	$E^{(2)}$ Kcal/mol	E(i) - E(j) (a.u)	F(i, j) (a.u)	CT (me)
Oryzenin-H_{30}…O_{49}	$n^{(1)}_{O_{29}} \rightarrow \sigma^{*}_{N_{51}\text{-}H_{52}}$	2.23	0.81	0.03	2.74
	$n^{(1)}_{Cl_{36}} \rightarrow \sigma^{*}_{C_{67}\text{-}H_{77}}$	2.51	1.06	0.047	3.93
	$n^{(4)}_{Cl_{36}} \rightarrow \sigma^{*}_{C_{67}\text{-}H_{77}}$	39.47	0.81	0.161	79.01
	$n^{(1)}_{O_{49}} \rightarrow \sigma^{*}_{O_{29}\text{-}H_{30}}$	8.61	1.03	0.084	13.30
	$n^{(2)}_{O_{49}} \rightarrow \sigma^{*}_{O_{29}\text{-}H_{30}}$	6.32	0.81	0.065	12.88
	$n^{(1)}_{O_{69}} \rightarrow \sigma^{*}_{C_{26}\text{-}H_{28}}$	3.18	0.99	0.05	5.10
Oryzenin-H_{30}…O_{91}	$n^{(1)}_{O_{29}} \rightarrow \sigma^{*}_{C_{78}\text{-}H_{89}}$	1.95	0.72	0.034	4.46
	$n^{(2)}_{Cl_{36}} \rightarrow \sigma^{*}_{O_{116}\text{-}H_{117}}$	2.7	1.17	0.051	3.80
	$n^{(2)}_{Cl_{36}} \rightarrow \sigma^{*}_{O_{119}\text{-}H_{120}}$	2.55	1.14	0.049	3.69
	$n^{(3)}_{Cl_{36}} \rightarrow \sigma^{*}_{O_{116}\text{-}H_{117}}$	10.08	0.7	0.075	22.96
	$n^{(3)}_{Cl_{36}} \rightarrow \sigma^{*}_{O_{119}\text{-}H_{120}}$	5.53	0.68	0.055	13.08
	$n^{(4)}_{Cl_{36}} \rightarrow \sigma^{*}_{O_{116}\text{-}H_{117}}$	18.01	0.8	0.109	37.13
	$n^{(4)}_{Cl_{36}} \rightarrow \sigma^{*}_{O_{119}\text{-}H_{120}}$	33.79	0.77	0.146	71.90
	$n^{(1)}_{O_{91}} \rightarrow \sigma^{*}_{O_{29}\text{-}H_{30}}$	9.99	1.08	0.093	14.83
	$n^{(2)}_{O_{119}} \rightarrow \sigma^{*}_{C_{26}\text{-}H_{28}}$	2.38	0.76	0.038	5.00
	$n^{(2)}_{S_{18}} \rightarrow \sigma^{*}_{C_{102}\text{-}H_{52}}$	1.60	0.67	0.033	4.85
	$n^{(1)}_{O_{29}} \rightarrow \sigma^{*}_{C_{41}\text{-}H_{50}}$	1.51	0.95	0.034	2.56
	$n^{(1)}_{O_{29}} \rightarrow \sigma^{*}_{C_{41}\text{-}H_{50}}$	2.42	0.69	0.037	5.75
	$n^{(1)}_{Cl_{36}} \rightarrow \sigma^{*}_{O_{93}\text{-}H_{94}}$	2.72	1.15	0.051	3.93
	$n^{(1)}_{Cl_{36}} \rightarrow \sigma^{*}_{O_{119}\text{-}H_{120}}$	1.52	1.13	0.038	2.26
	$n^{(2)}_{Cl_{36}} \rightarrow \sigma^{*}_{C_{80}\text{-}H_{95}}$	5.67	0.69	0.056	13.17
	$n^{(3)}_{Cl_{36}} \rightarrow \sigma^{*}_{C_{93}\text{-}H_{94}}$	5.69	0.71	0.057	12.89
Oryzenin H_{30}…O_{99}	$n^{(2)}_{S_{18}} \rightarrow \sigma^{*}_{C_{102}\text{-}H_{52}}$	1.60	0.67	0.033	4.85
	$n^{(1)}_{O_{29}} \rightarrow \sigma^{*}_{C_{41}\text{-}H_{50}}$	1.51	0.95	0.034	2.56
	$n^{(1)}_{O_{29}} \rightarrow \sigma^{*}_{C_{41}\text{-}H_{50}}$	2.42	0.69	0.037	5.75
	$n^{(1)}_{Cl_{36}} \rightarrow \sigma^{*}_{O_{93}\text{-}H_{94}}$	2.72	1.15	0.051	3.93
	$n^{(1)}_{Cl_{36}} \rightarrow \sigma^{*}_{O_{119}\text{-}H_{120}}$	1.52	1.13	0.038	2.26
	$n^{(2)}_{Cl_{36}} \rightarrow \sigma^{*}_{C_{80}\text{-}H_{95}}$	5.67	0.69	0.056	13.17
	$n^{(3)}_{Cl_{36}} \rightarrow \sigma^{*}_{C_{93}\text{-}H_{94}}$	5.69	0.71	0.057	12.89
	$n^{(3)}_{Cl_{36}} \rightarrow \sigma^{*}_{O_{96}\text{-}H_{97}}$	1.88	0.75	0.034	4.11
	$n^{(3)}_{Cl_{36}} \rightarrow \sigma^{*}_{O_{119}\text{-}H_{120}}$	8.52	0.69	0.069	20.00
	$n^{(4)}_{Cl_{36}} \rightarrow \sigma^{*}_{C_{93}\text{-}H_{94}}$	20.82	0.81	0.117	41.73
	$n^{(4)}_{Cl_{36}} \rightarrow \sigma^{*}_{O_{119}\text{-}H_{120}}$	21.81	0.79	0.118	44.62
	$n^{(1)}_{O_{54}} \rightarrow \sigma^{*}_{C_{19}\text{-}H_{22}}$	2.78	1.04	0.048	4.26

Continued

	$n^{(2)}_{O_{54}} \rightarrow \sigma^{*}_{C_{23}\text{-}H_{25}}$	3.26	0.8	0.046	6.6
	$n^{(1)}_{O_{99}} \rightarrow \sigma^{*}_{O_{29}\text{-}H_{30}}$	10.14	0.99	0.09	16.53
	$n^{(2)}_{O_{99}} \rightarrow \sigma^{*}_{O_{29}\text{-}H_{30}}$	3.38	0.86	0.048	6.23
$N_9H_{10}\ldots O_{49}$	$n^{(1)}_{O_{49}} \rightarrow \sigma^{*}_{N_9\text{-}H_{10}}$	1.67	1.00	0.037	2.74
	$n^{(2)}_{O_{49}} \rightarrow \sigma^{*}_{N_9\text{-}H_{10}}$	5.33	0.76	0.057	11.25
	$n^{(3)}_{O_{74}} \rightarrow \sigma^{*}_{C_{11}\text{-}H_{13}}$	2.87	0.78	0.042	5.80
$N_9\text{-}H_{10}\ldots O_{91}$	$n^{(1)}_{Cl_{36}} \rightarrow \sigma^{*}_{O_{51}\text{-}H_{52}}$	1.93	1.16	0.043	2.75
	$n^{(1)}_{Cl_{36}} \rightarrow \sigma^{*}_{O_{54}\text{-}H_{123}}$	2.39	1.13	0.048	3.61
	$n^{(2)}_{Cl_{36}} \rightarrow \sigma^{*}_{O_{51}\text{-}H_{52}}$	2.82	0.7	0.04	6.53
	$n^{(2)}_{Cl_{36}} \rightarrow \sigma^{*}_{O_{54}\text{-}H_{123}}$	1.57	0.67	0.029	3.75
	$n^{(3)}_{Cl_{36}} \rightarrow \sigma^{*}_{O_{51}\text{-}H_{52}}$	8.09	0.69	0.067	18.86
	$n^{(3)}_{Cl_{36}} \rightarrow \sigma^{*}_{O_{54}\text{-}H_{123}}$	3.09	0.66	0.041	7.72
	$n^{(4)}_{Cl_{36}} \rightarrow \sigma^{*}_{O_{51}\text{-}H_{52}}$	17.94	0.81	0.109	36.22
	$n^{(4)}_{Cl_{36}} \rightarrow \sigma^{*}_{O_{54}\text{-}H_{123}}$	28.98	0.78	0.135	59.91
	$n^{(1)}_{O_{54}} \rightarrow \sigma^{*}_{C_4\text{-}H_8}$	5.59	0.77	0.059	11.74
	$n^{(1)}_{O_{91}} \rightarrow \sigma^{*}_{N_9\text{-}H_{10}}$	4.99	1.04	0.064	7.57
	$n^{(1)}_{O_{119}} \rightarrow \sigma^{*}_{C_{11}\text{-}H_{13}}$	1.58	1.08	0.037	2.35
$N_9\text{-}H_{10}\ldots O_{99}$	$n^{(1)}_{O_{42}} \rightarrow \sigma^{*}_{N_9\text{-}H_{10}}$	1.54	1.01	0.035	2.40
	$n^{(1)}_{O_{99}} \rightarrow \sigma^{*}_{N_9\text{-}H_{10}}$	7.24	1.02	0.077	11.40
	$n^{(2)}_{O_{99}} \rightarrow \sigma^{*}_{N_9\text{-}H_{10}}$	1.83	0.75	0.033	3.87

between the energies of NBO electron donors (i) and NBO electron acceptor (j). They also show the elements F(i, j) of the Fock matrix and the CT. The model of the latter, constructed by Reed and al [11], makes it possible to describe the interactions in the AMP3G-oryzenin and AMP4G-oryzenin complexes.

3.1. NBO Analysis of the Amylopectin (AMP3G/AMP4G)-Oryzenin Complexes

The NBO analysis presents the results for which the stabilization energies are greater than 1.5 kcal·mol^{-1}. CT are correlated with these quantities. The relative positions of the interacting elements influence them. In the AMP3G-oryzenin complex, for the oryzenin-$H_{30}\ldots O_{49}$ and oryzenin-$H_{30}\ldots O_{99}$ interactions, the most important contributions to equilibrium result from the transfer of free chlorine pairs from oryzenin. They correspond to the transitions:

– For the interaction oryzenin-$H_{30}\ldots O_{49}$:

- $n^{(4)}_{Cl_{36}} \rightarrow \sigma^{*}_{C_{69}\text{-}H_{77}}$ with $E^{(2)}$ = 51.82 kcal·mol^{-1} and CT = 117.37 me

– For oryzenin-$H_{30}\ldots O_{99}$:

- $n^{(4)}_{Cl_{36}} \rightarrow \sigma^{*}_{O_{91}\text{-}H_{102}}$ with $E^{(2)}$ = 38.5 kcal·mol^{-1} and CT = 76.10 me.

A secondary stabilization exists; it's based on the following transitions:

– For oryzenin-H_{30}…O_{49},

- $n_{O_{49}}^{(2)} \rightarrow \sigma_{O_{29}\text{-}H_{30}}^{*}$ with $E^{(2)}$ = 8.46 kcal·mol^{-1} and CT = 16.73 me

– For oryzenin-H_{30}…O_{99},

- $n_{O_{99}}^{(2)} \rightarrow \sigma_{O_{29}\text{-}H_{30}}^{*}$ with E $^{(2)}$ = 10.59 kcal·mol^{-1} and CT = 20.98 me

The CT of 20.98 suggests to me that the strong HB in AMP3G-oryzenin comes from the oryzenin-H_{30}…O_{99} interaction. For those with the N_9H_{10} of oryzenin, no CT is observed with chlorine. Its position prohibits it within the complexes. The most important transfers are those concerning O_{49} and N_9-H_{10} bonds. They're

– For the interaction N_9-H_{10}…O_{49},

- $n_{O_{49}}^{(1)} \rightarrow \sigma_{N_9\text{-}H_{10}}^{*}$ with $E^{(2)}$ = 5.96 kcal·mol^{-1} and CT = 9.24 me

– For the interaction N_9-H_{10}…O_{99},

- $n_{O_{99}}^{(1)} \rightarrow \sigma_{N_9\text{-}H_{10}}^{*}$ with $E^{(2)}$ = 8.59 kcal·mol^{-1} and CT = 17.55 me.

In the case of the AMP4G-oryzenin complex, the strongest stabilization comes from free chlorine pairs:

– For the interaction oryzenin-H_{30}…O_{49},

- $n_{Cl_{36}}^{(4)} \rightarrow \sigma_{C_{69}\text{-}H_{77}}^{*}$ with $E^{(2)}$ = 39.47 kcal·mol^{-1} and CT = 79.01 me

– For the interaction oryzenin-H_{30}…O_{91},

- $n_{Cl_{36}}^{(4)} \rightarrow \sigma_{O_{119}\text{-}H_{120}}^{*}$ transition with $E^{(2)}$ = 33.79 kcal·mol^{-1} CT = 71.90 me

– For oryzenin-H_{30}…O_{99}, two transitions of chlorine bring the strongest stabilization. It's about:

- $n_{Cl_{36}}^{(4)} \rightarrow \sigma_{C_{93}\text{-}H_{94}}^{*}$ with $E^{(2)}$ = 20.82 kcal·mol^{-1} and CT = 41.73 me
- $n_{Cl_{36}}^{(4)} \rightarrow \sigma_{O_{119}\text{-}H_{120}}^{*}$ with $E^{(2)}$ = 21.81 kcal·mol^{-1} and CT = 44.62 me

Besides, the stabilization brought mainly by chlorine, there's a secondary one. This result from transitions:

– For oryzenin-H_{30}…O_{49},

- $n_{O_{49}}^{(1)} \rightarrow \sigma_{O_{29}\text{-}H_{30}}^{*}$ with $E^{(2)}$ = 8.61 kcal·mol^{-1} and CT = 13.30 me
- $n_{O_{49}}^{(2)} \rightarrow \sigma_{O_{29}\text{-}H_{30}}^{*}$ with $E^{(2)}$ = 6.32 kcal·mol^{-1} and CT = 12.88 me

– For oryzenin-H_{30}…O_{91},

- $n_{O_{91}}^{(1)} \rightarrow \sigma_{O_{29}\text{-}H_{30}}^{*}$ with $E^{(2)}$ = 9.99 kcal·mol^{-1} and CT = 14.83 me.

– For oryzenin-H_{30}…O_{99},

- $n_{O_{91}}^{(1)} \rightarrow \sigma_{O_{29}\text{-}H_{30}}^{*}$ with $E^{(2)}$ = 10.14 kcal·mol^{-1} and CT = 16.53 me.

Oxygen O_{99} participates more in CT. The corresponding value is 16. This proves that the stabilization is maximum for the transition which concerns it. Under these conditions, the oryzenin H_{30}…O_{99} interaction becomes the most probable. Regarding N_9H_{10}…O_{49}, no stabilization comes from chlorine. CT results from transition:

- $n_{O_{49}}^{(2)} \rightarrow \sigma_{N_9\text{-}H_{10}}^{*}$ with $E^{(2)}$ = 5.33 kcal·mol^{-1} and CT = 11.25 me.

– For N_9H_{10}…O_{91}, two transitions from the chlorine atom provide the solidest stabilization. They are

- $n_{Cl_{36}}^{(4)} \rightarrow \sigma_{O_{54}\text{-}H_{123}}^{*}$ with $E^{(2)}$ = 28.98 kcal·mol^{-1} and CT = 59.91 me
- $n_{Cl_{36}}^{(4)} \rightarrow \sigma_{O_{51}\text{-}H_{52}}^{*}$ with $E^{(2)}$ = 17.94 kcal·mol^{-1} and CT = 36.22 me

– For the interaction N_9-H_{10}…O_{99}:

- $n_{O_{99}}^{(1)} \rightarrow \sigma^{*}_{N_9\text{-}H_{10}}$ with $E^{(2)} = 7.24$ kcal·mol^{-1} and CT = 11.40 me.

HB is strong with the oryzenin-H30 probe associated with O_{99} in the AMP3G and in AMP4G complexes. This interaction results from the lone chlorine pairs of oryzenin. It initiates the transformation of amylopectin at its branching level. The research exploits this result to construct the ideal complexes. It uses it to model the interactions between oryzenin and AMP4G or AMP3G. In previous research [2], the electrostatic potential of molecular interaction sites indicated that the oryzenin H_{30} and H_{10} constitute the highest potential $V_{S,max}$. This work appropriates this result to study AMP3G.

3.2. Interaction AMP3G-Oryzenine

These atoms illustrate the hydrogen donor potential of the oryzenin. The geometrical, energetic, spectroscopic parameters and the NBO analysis relate to the interactions involving this hydrogen. **Figure 1** shows the geometries of the optimized complexes. A red ball represents an oxygen atom. A big white corresponds to a carbon. A small one schematizes hydrogen.

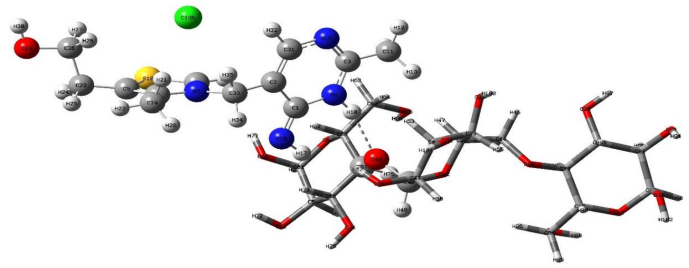

(a)

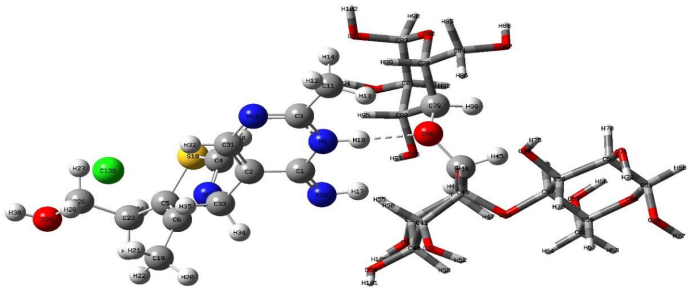

(b)

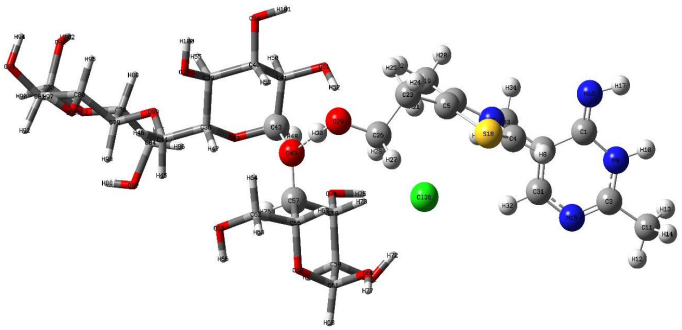

(c)

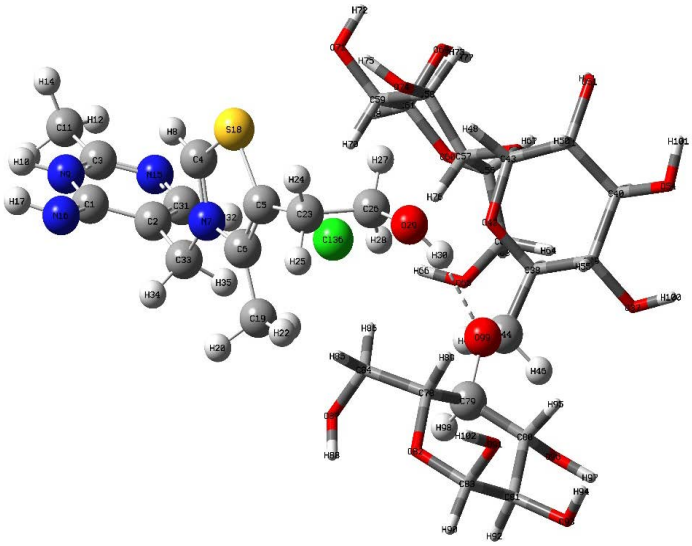

(d)

Figure 1. 3D structures of optimized AMP4G-oryzenin. (a) Interaction $N_9H_{10}\ldots O_{49}$; (b) Interaction $N_9H_{10}\ldots O_{99}$; (c) Interaction $N_9H_{10}\ldots O_{99}$; (d) Interaction oryzenin-H30…O_{99}.

Table 3 shows the geometric parameters. It presents the distance *d*, the angles of linearity α and of direction β associated with HB. The distance *d* varies from 1.92 Å to 2.17 Å [20]. It characterizes HB. They're less than 2.62 Å [21] [22]; this value defines the Vander Waals sum radii of the hydrogen and oxygen atoms [23] [24]. Oryzenin-$H_{30}\ldots O_{49}$, oryzenin-$H_{30}\ldots O_{99}$ and $N_9H_{10}\ldots O_{99}$ respect the condition for HB [24]. On the other hand, the α and β associated with the $N_9H_{10}\ldots O_{49}$ interaction deviate from the ideal values. These geometrical parameters establish that oryzenin-$H_{30}\ldots O_{99}$ is the strongest HB.

Table 4 shows the variations of the enthalpy, the entropy and the free enthalpy of reaction linked to the interactions between AMP3G and oryzenin. Those relating to the enthalpies of reaction are all negative. They fluctuate between -2.730 kcal·mol^{-1} and -20.175 kcal·mol^{-1}. These values suggest that all reactions are exothermic. Those associated with the oryzenin-$H_{30}\ldots O_{99}$ interaction represent the weakest.

This interaction corresponds to the most stable. Its free enthalpy of reaction ($\Delta rG = -5.30$ kcal·mol^{-1}) indicates that its formation is spontaneous. The other interactions ($N_9H_{10}\ldots O_{49}$ and $N_9H_{10}\ldots O_{99}$) are exothermic but not spontaneous ($\Delta rG > 0$). **Figure 2** shows free enthalpies of reaction changes associated with AM3G-oryzenin and AMP3G-oryzenin complexes. It illustrates that the others ($N_9H_{10}\ldots O_{49}$ and $N_9H_{10}\ldots O_{99}$) aren't spontaneous ($ArG > 0$).

These results suggest the degradation modality of amylopectin; this process begins with the establishment of HB oryzenin-$H_{30}\ldots O_{99}$. It breaks the osidic bridges of the ramification. It leads to the formation of amyloidosis. Its production linked to this process and its natural disappearance [2] occurs concomitantly. They explain the slow decrease in its rate presence in the starch during the aging of the rice. Furthermore, spectroscopic parameters precise this finding.

Table 3. Geometric parameters of the AMP3G-oryzenine complex at ONIOM (B3LYP/6-31+G(d, p): AM1).

HB AMP3G-oryzenin	d (Å)	α (°)	β (°)
oryzenin-H_{30}…O_{49}	1.93	172.3	104.2
oryzenin-H_{30}…O_{99}	1.92	177.0	109.1
N_9-H_{10}…O_{49}	2.17	162.6	116.1
N_9-H_{10}…O_{99}	1.99	172.7	108.9

Table 4. Energetic parameters of AMP3G-oryzenine complex at ONIOM (B3LYP/6-31+G(d, p): AM1).

HB AMP3G-oryzenin	ΔrH (kcal·mol^{-1})	ΔrS (kcal·K^{-1}·mol^{-1})	ΔrG (kcal·mol^{-1})
oryzenin-H_{30}…O_{49}	−19.126	−0.046	−5.342
oryzenin-H_{30}…O_{99}	−20.175	−0.050	−5.300
N_9-H_{10}…O_{49}	−2.730	−0.039	9.362
N_9-H_{10}…O_{99}	−4.865	−0.041	6.811

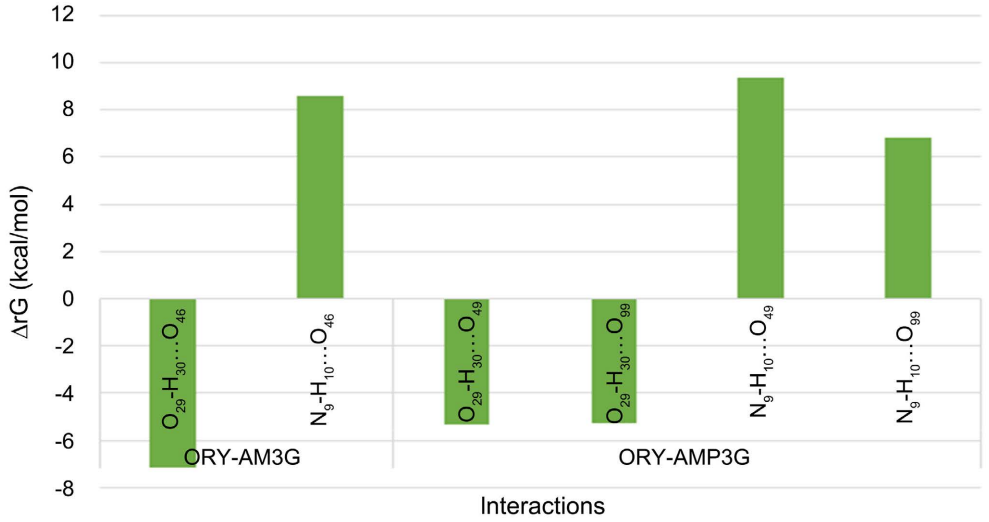

Figure 2. Free enthalpies of reaction changes associated with AM3G-oryzenine and AMP3G-oryzenin complex.

Table 5 outlines the O-H and N-H stretching frequency shift of free and complex oryzenin. It presents their differences. These reach 281 cm^{-1} for oryzenin-H_{30}…O_{99} interaction and 236 cm^{-1} for oryzenin-H_{30}…O_{49}. Those of the N-H bonds remain lower than them. They only attain 126 cm^{-1} for HB N_9-H_{10}…O_{49}. Important variation in vibrational frequencies reflects the strong oxygen attraction of the O_{99} osidic bridge around H_{30}. It's greater for the O-H bond; it reaches 281 cm^{-1} for oryzenin-H_{30}…O_{99}. It reveals that H_{30} exerts its strongest attraction on oxygen O_{99} of the amylopectin branching osidic bridge. The latter breaks. This rupture leads to linear chains of α-D-glucose or amyloidosis. This result suggests that the degradation of amylopectin is easier than that of amylose.

Table 5. Elongation frequencies and its variations (cm^{-1}) associated with O-H and N-H of free and complex oryzenin in the AMP4G-oryzenin interaction.

HB AMP3G-oryzenin	Free oryzenin		Complex oryzenin		Variations $\Delta\upsilon$free-$\Delta\upsilon$complex		$\Delta\upsilon$ (AM3G-oryzenin)-$\Delta\upsilon$ (AMP3G-oryzenin)	
	O-H	N-H	O-H	N-H	O-H	N-H	O-H	N-H
Oryzenin-H_{30}…O_{49}	3839		3603		236		75	
Oryzenin-H_{30}…O_{99}	3839		3558		281		120	
N_9-H_{10}…O_{49}		3591		3465		126		19
N_9-H_{10}…O_{99}		3591		3375		216		109

The rupture of its osidic bridge conducts to the formation of this starch latter component. This result refutes the conclusions of [3]. Its authors conjecture that the storage of rice favours the fall in the proportion of amylose in the starch; they affirm that an increase in that of amylopectin in the same proportion simultaneously. Thus, degradation of rice starch changes the amylose-amylopectin ratio. This result corroborates the observations of Cao and al [25] regarding the variation over time of this latter. The first degradation of amylopectin also supports the conclusions drawn from the analysis of geometric, energetic, and spectroscopy. Moreover, this research concerns the AMP4G-oryzenin complex.

3.3. Interaction AMP4G-Oryzenin

This section presents and discusses the results related to the geometrical, energetic, spectroscopic parameters and NBO analysis of the AMP4G-oryzenin complexes. The optimized geometries (**Figure 3**) show three osidic bridges (O_{49}, O_{91}, O_{99}) of the four α-D-glucose "synthons" representing the portion of amylopectin interacting with the two main oryzenin interaction sites (oryzenin-H_{30} and N_9-H_{10}). The distance d materialized by a dotted line in each complex indicates the interaction between the two sites. The geometrical parameters allow identifying it.

Table 6 shows the geometric parameters (d, α, β) of the interactions characterizing HB in the AMP4G-oryzenin complex. Its data agree with those established by Desiraju and al [22]. They indicate that the oryzenin-H_{30}…O_{49} and oryzenin-H_{30}…O_{91} interactions lead to strong HB; their distances d are very close (1.93 Å; 1.94 Å).

The environment around the HB influences the angular parameters. The linearity angle α of the oryzenin-H_{30}…O_{91} interaction equals 170.8˚. It reaches 172.4˚ for oryzenin-H_{30}…O_{49}. The angles α deviate from their ideal values, 180˚. β, associated oryzenin-H_{30}…O_{49} interaction, is 5.1˚ lower than the expected 109.9˚. The β angle of the oryzenin-H_{30}…O_{99} interaction exceeds it by 0.6. It's at the upper limit of the interval of Desiraju and al [22]. These two angles β are different from 109.9˚. Analysis of the three geometric parameters suggests that HB H_{30}…O_{91} is the most stable of the AMP4G-oryzenin complex.

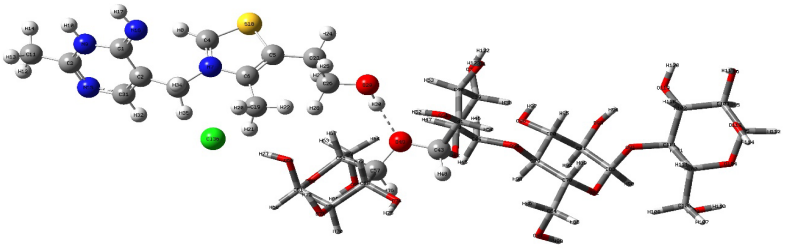

(a)

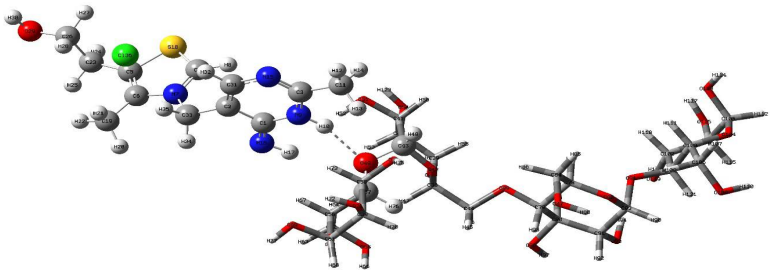

(b)

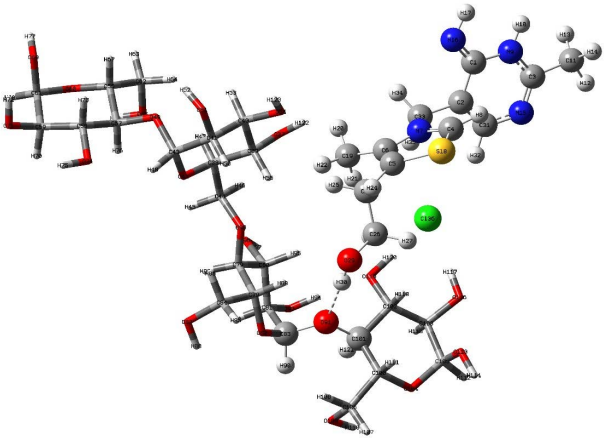

(c)

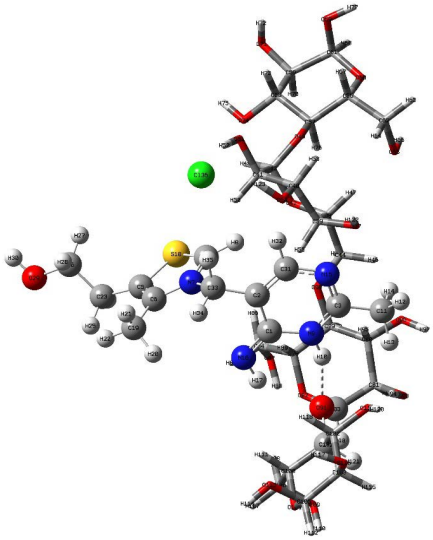

(d)

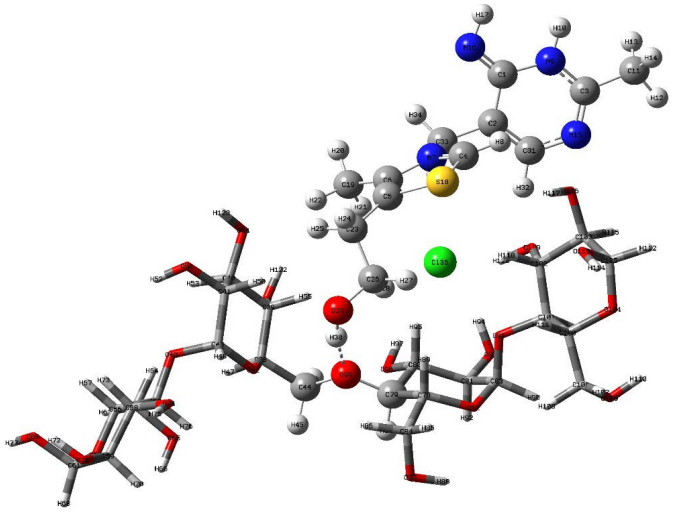

(e)

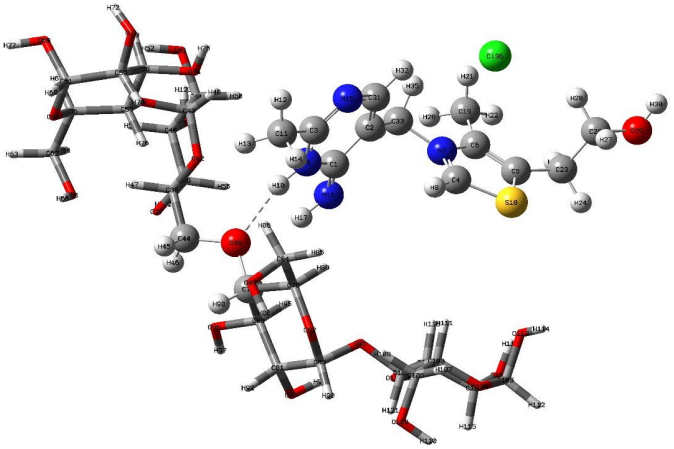

(f)

Figure 3. 3D structures of optimized AMP4G-oryzenin. (a) oryzenin-H_{30}…O_{49} interaction; (b) oryzenin-N_9H_{10}…O_{49} interaction; (c) oryzenin-H_{30}…O_{91} interaction; (d) Oryzenin N_9H_{10}…O_{91} interaction; (e) oryzenin-H_{30}…O_{99} interaction; (f) Interaction N_9H_{10}…O_{99}.

Table 6. Geometrical parameters of the AMP4G-oryzenin complex at ONIOM (B3LYP/6-31+G(d, p): AM1).

HB AMP4G-oryzenin		d (Å)	α (°)	β (°)
Oryzenin-H_{30}	O_{49}	1.93	172.4	104.4
	O_{91}	1.94	170.8	110.1
	O_{99}	1.89	160.6	119.5
N_9-H_{10}	O_{49}	2.16	161.6	107.6
	O_{91}	2.18	159.7	98.3
	O_{99}	2.07	161.1	121.1

Its distance d respects the criterion of Desiraju and al [22]. Its angle α and β remain close to their ideal values. These parameters lead to the conclusion that

the AMP4G degradation begins in O_{91} locate on osidic bridge position α (1, 6).

Table 7 compiles the variation of the enthalpies, entropy, and free enthalpies for AMP4G-oryzenin interactions. The variations of the enthalpies are all negative. They appear between −3.525 kcal·mol^{-1} and −27.968 kcal·mol^{-1}; The HB formation is exothermic. The ΔrH also suggest that the interactions created by oryzenin-H_{30} and N_9H_{10} are all stable. The lowest ΔrH corresponds to the interaction oryzenin-H_{30}…O_{99} (ΔrH = −27.968 kcal·mol^{-1}).

The negative ΔrG values with oryzenin-H_{30} show that the interactions oryzenin-H_{30}…O_{49}, oryzenin-H_{30}…O_{91} and oryzenin-H_{30}…O_{99} are spontaneous while those established with N_9H_{10} aren't. ΔrG coincides with the bottommost value (ΔrG = −9.719 kcal·mol^{-1}) for the interaction oryzenin-H_{30}…O_{99}. This latter is the strongest HB and the most spontaneous. The HB with O_{49} and O_{91} aren't negligible. These results indicate that the O_{99} site is the most favourable for HB formation. This suggests that AMP4G degrade primarily from this site.

Table 8 shows the υ(O-H) and υ(N-H) stretching frequencies of free and associated oryzenin. The stretch frequency changes are all positive. The strengths of HB linked with them decrease in the order O_{99}, O_{91} and O_{49} for AMP4G. They correspond to the most stable interactions between AMP4G and oryzenin-H_{30}; the most important variation is those related to the oryzenin-H_{30}…O_{99} interaction of 261 cm^{-1}. It proves that the latter is the strongest of this group.

The O_{99} site is the most favourable for the formation of HB. This suggests that AMP4G mostly breaks down from there. Its deterioration begins with this osidic bridge in position α (1.6). The rupture of the latter promotes the formation of linear α-D-glucose chains; it leads to amyloidosis. These consist of tetra saccharides. They degrade according to the mechanism described by [2]. Then, this work elucidates the mechanism of starch degradation following the appearance of amyloidosis.

Figure 4 shows the free enthalpy changes associated with interactions between $O_{29}H_{30}$ or N_9H_{10} and the appropriate proton acceptor sites of AM4G and AMP4G. Its data reveal that all variations linked to AM4G and AMP4G are negative for the $O_{29}H_{30}$ probe. The modifications related to the interactions between N9H10 and AM4G are also. The formation of HB following oryzenin-$O_{29}H_{30}$-AMP4G or

Table 7. Energetic parameters of AMP4G-oryzenin complexes at ONIOM (B3LYP/6-31+G(d, p): AM1).

AMP4G-ORY HB with osidic bridges		ΔrH (kcal·mol^{-1})	ΔrS (kcal·K^{-1}·mol^{-1})	ΔrG (kcal·mol^{-1})
oryzenin-H_{30}	O_{49}	−18.997	−0.046	−5.273
	O_{91}	−19.997	−0.059	−2.418
	O_{99}	−27.968	−0.061	−9.719
N_9-H_{10}	O_{49}	−3.525	−0.038	7.702
	O_{91}	−17.394	−0.062	0.998
	O_{99}	−9.896	−0.047	4.016

Table 8. Elongation frequencies and changes in O-H and N-H elongation frequencies (cm^{-1}) free and complex oryzenin from AMP4G-oryzenin interactions.

HB AMP4G-oryzenin	ΔυFree oryzenin		ΔυComplex oryzenin		Δυfree-Δυcomp		Δυ AM4G-ΔυAMP 4G			
	O-H	N-H	O-H	N-H	O-H	N-H	O-H		N-H	
Oryzenin-H_{30}…O_{49}	3839		3600		239		O(1)	−48		
							O(2)	−11		
Oryzenin-H_{30}…O_{91}	3839		3582		257		O(1)	−30		
							O(2)	7		
oryzenin-H_{30}…O_{99}	3839		3578		261		O(1)	−26		
							O(2)	11		
N_9-H_{10}…O_{49}		3591		3439		152			O(1)	70
									O(2)	−60
N_9-H_{10}…O_{91}		3591		3449		142			O(1)	60
									O(2)	−71
N_9-H_{10}…O_{99}		3591		3394		197			O(1)	115
									O(2)	−16

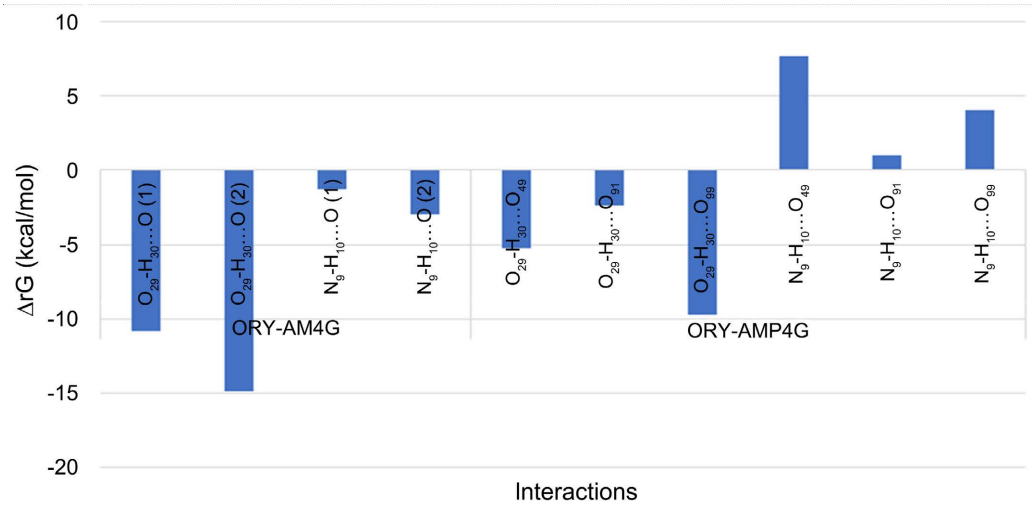

Figure 4. AM4G-oryzenin and AMP4G-oryzenin free enthalpy variations.

oryzenin-N_9H_{10}-AM4G interactions correspond to spontaneous processes for the osidic bridges O_{49}, O_{91}, O_{99} polysaccharides. On the other hand, the positive values associated with the free enthalpy demonstrate that the interactions of oryzenin-N_9H_{10}-AMP4G aren't. This energetic component hardly sheds light on the complete mechanism underlying the degradation of AMP4G.

The interactions between two polysaccharides with $O_{29}H_{30}$ lead spontaneously to the formation of HB with each osidic bridge O_{49}, O_{91}. O_{99}. In other words, their thermodynamic similarity doesn't make it possible to detect the second stage of the AMP4G disintegration during its progressive transformation into AM4G. This limit justifies the choice of spectroscopy. This can explain degrada-

tion order of the two saccharides in this phase deterioration; the local nature of the phenomenon pleads for this approach.

For the same oryzenin-H_{30} probe, the two oxygen osidic bridges O(1) and O(2) possible for the oryzenin-H_{30}…O_{91} interaction, the difference in frequency between the free and associated forms is 257 cm^{-1}. Moreover, that between AM4G and AMP4G is −30 cm^{-1} for O(1) and +7 cm^{-1} around O(2) as the receptor site. The frequency variation is greater for amylopectin near O(1) compared to amyloidosis. It reflects a stronger attraction of oxygen from the osidic bridge oxygen O_{91} towards H_{30}. It breaks the latter more easily.

The degradation of amylopectin into amylose is carried out continuously when the first interact with O_{91}. The same reasoning leads to similar conclusions with O_{99} and O_{49}. In the latter case, the transformation of AMP4G takes place around O(1) mainly; a smaller proportion comes from its O(2). Furthermore, this research extends to NBO analysis of the AMP4G-oryzenin and AMP3G-oryzenin complexes.

4. Conclusions

This work aims to clarify the chemical processes underlying the degradation of amylopectin with oryzenin. It exploits resources from quantum chemistry as a method. It uses NBO analysis and calculates the geometric, energetic, and spectroscopic parameters of the AMP3G-oryzenin and AMP4G-oryzenin complexes. It employs the ONIOM [DFT/B3LYP/6-31+G(d, p): AM1]. This method makes it possible to suggest a mechanism to explain the degradation of amylopectin by oryzenin. This latter establishes HB through H_{30} or H_{10}.

This work locates the presence of HB near the oxygen of AMP3G or AMP4G situated at α (1, 6) on the osidic bridge O_{99}. The latter coincides with their branching points. HB results from the strong attraction of oxygen O_{99} to H_{30}. It causes the rupture of this bridge. It leads to the formation of amyloid. On the other hand, the frequency variation is greater for amylopectin around O(1); it exceeds that associated with the interaction with amyloidosis near O(2). This difference reflects a stronger attraction of oxygen O_{99}, O_{91} or O_{49} towards H_{30}. It suggests that the degradation of amylopectin is easier than that of amylose. So, these forces readily break the branching of amylopectin. Its degradation into amyloid becomes continuous. The latter deteriorates gradually according to the mechanism described by [2]; its products are monosaccharides and disaccharides during rice aging or storage. This finding contributes to the debate on rice starch degradation; it refutes the conclusions of [3].

According to [3], the storage of rice promotes a reduction in the proportion of amylose in the starch; it causes an equivalent increase in that of amylopectin. On the other hand, the observations of Cao *et al.* [25] confirm the findings of this research. These authors state that amylopectin is degraded before amyloidosis. Moreover, research reinforces the team's findings [2]. It specifies that the deterioration of rice starch begins with that of its amylopectin. Therefore, it explains

the origin of disaccharides and monosaccharides during the aging of rice. Their presence is linked to two types of amyloidosis. Some of it comes from the continual breakdown of amylopectin. The other relates to amyloid, a constituent of starch. Moreover, the article highlights the main difference between amylopectin and amyloid regarding action of oryzenin.

The attraction of oxygen from the saccharide bridge by H_{30} differs between amylopectin-oryzenin and amyloid-oryzenin. The O-H stretching frequency difference associated with it exceeds that of the second complex. Simply, the attraction of the oryzenin's H_{30} for amylopectin's oxygen on the osidic bridge remains higher than that observed for amyloid. This result constitutes further evidence that amylopectin degrades before amyloid in rice starch.

Conflicts of Interest

The authors declare no conflict of interest regarding the publication of this paper.

References

[1] Koffi, K.A., N'Guessan, R.B. and Bamba, E.H.S. (2021) The Phospholipid Degradation in Paddy Rice: A Theoretical Model with DFT/B3LYP 6-311 G. *European Journal of Applied Sciences*, **9**, 162-174. https://doi.org/10.14738/aivp.95.10897

[2] N'guessan, B.R., Bamba, E.H.S. and Koffi, K.A. (2022) The Oryzenin's Effect on Di, Tri and Quadri-Saccharide Degradation. An Investigation by a Mixed Method: ONIOM (DFT/B3LYP/6-31 + G(d, p): AM1). *Computational Chemistry*, **10**, 97-119. https://doi.org/10.4236/cc.2022.102005

[3] Abeysundara, A., Navaratne, S., Wickramasinghe, I. and Ekanayake, D. (2017) Determination of Changes of Amylose and Amylopectin Content of Paddy during Early Storage. *International Journal of Science and Research*, **6**, 2094-2097. https://doi.org/10.21275/ART20164500

[4] Cipcigan, F., Sokhan, V., Martyna, G. and Crain, J. (2018) Structure and Hydrogen Bonding at the Limits of Liquid Water Stability. *Scientific Reports*, **8**, Article No. 1718. https://doi.org/10.1038/s41598-017-18975-7

[5] Liu, J., He, X., Zhang, J.Z.H. and Qi, L.-W. (2018) Hydrogen-Bond Structure Dynamics in Bulk Water: Insights from *ab Initio* Simulations with Coupled Cluster Theory. *Chemical Science*, **9**, 2065-2073. https://doi.org/10.1039/C7SC04205A

[6] Arno, B., Layton, M.L. and Kathleen, K.V. (2000) Hydrogen Bonds in Carboxylic Acid-Carboxylate Systems in Solution. 1. In Anhydrous, Aprotic Media. *Organic Letters*, **2**, 2007-2009. https://doi.org/10.1021/ol005776j

[7] Zhang, Q. and Du, L. (2016) Hydrogen Bonding in the Carboxylic Acid-Aldehyde Complexes. *Computational and Theoretical Chemistry*, **1078**, 123-128. https://doi.org/10.1016/j.comptc.2016.01.007

[8] Weinhold, F. (2012) Natural Bond Orbital Analysis: A Critical Overview of Relationships to Alternative Bonding Perspectives. *Journal of Computational Chemistry*, **33**, 2363-2379. https://doi.org/10.1002/jcc.23060

[9] Behzadi, H., Esrafili, M.D. and Hadipour, N.L. (2007) A Theoretical Study of 17O, 14N and 2H Nuclear Quadrupole Coupling Tensors in the Real Crystalline Structure of Acetaminophen. *Chemical Physics*, **333**, 97-104. https://doi.org/10.1016/j.chemphys.2007.01.011

[10] Esrafili, M.D., Behzadi, H. and Hadipour, N.L. (2008) 14N and 17O Electric Field Gradient Tensors in Benzamide Clusters: Theoretical Evidence for Cooperative and Electronic Delocalization Effects in N-H···O Hydrogen Bonding. *Chemical Physics*, **348**, 175-180. https://doi.org/10.1016/j.chemphys.2008.02.056

[11] Reed, A.E., Curtiss, L.A. and Weinhold, F. (1988) Intermolecular Interactions from a Natural Bond Orbital, Donor-Acceptor Viewpoint. *Chemical Reviews*, **88**, 899-926. https://doi.org/10.1021/cr00088a005

[12] Dapprich, S., Komáromi, I., Byun, K.S., Morokuma, K. and Frisch, M.J. (1999) A New ONIOM Implementation in Gaussian98. Part I. The Calculation of Energies, Gradients, Vibrational Frequencies and Electric Field Derivatives. *Journal of Molecular Structure*: *THEOCHEM*, **461**-**462**, 1-21. https://doi.org/10.1016/S0166-1280(98)00475-8

[13] Vreven, T., Byun, K.S., Komáromi, I., Dapprich, S., Montgomery, J.A., Morokuma, K. and Frisch, M.J. (2006) Combining Quantum Mechanics Methods with Molecular Mechanics Methods in ONIOM. *Journal of Chemical Theory and Computation*, **2**, 815-826. https://doi.org/10.1021/ct050289g

[14] Frisch, M.J., Trucks, G.W., Schlegel, H.B., *et al.* (2009) Gaussian 09, Revision A.02. Gaussian, Inc., Wallingford.

[15] Günay, N., Pir, H., Avcı, D. and Atalay, Y. (2013) NLO and NBO Analysis of Sarcosine-Maleic Acid by Using HF and B3LYP Calculations. *Journal of Chemistry*, **2013**, Article ID: 712130. https://doi.org/10.1155/2013/712130

[16] Murray, J.S. and Sen, K. (1996) Molecular Electrostatic Potentials: Concepts and Applications. Elsevier, Amsterdam, 105-538. https://doi.org/10.1016/S1380-7323(96)80042-2

[17] Brinck, T. (1998) The Use of the Electrostatic Potential for Analysis and Prediction of Intermolecular Interactions. *Theoretical and Computational Chemistry*, **5**, 51-93. https://doi.org/10.1016/S1380-7323(98)80005-8

[18] Demircioğlu, Z., Albayrak, Ç. and Büyükgüngör, O. (2014) Theoretical and Experimental Investigation of (E)-2-([3,4-dimethylphenyl)imino]methyl)-3-methoxyphenol: Enol-keto Tautomerism, Spectroscopic Properties, NLO, NBO and NPA Analysis. *Journal of Molecular Structure*, **1065**-**1066**, 210-222. https://doi.org/10.1016/j.molstruc.2014.02.062

[19] Bader, R.F.W., Carroll, M.T., Cheeseman, J.R. and Chang, C. (1987) Properties of Atoms in Molecules: Atomic Volumes. *Journal of the American Chemical Society*, **109**, 7968-7979. https://doi.org/10.1021/ja00260a006

[20] Arunan, E., Desiraju, G.R., Klein, R.A., Sadlej, J., Scheiner, S., Alkorta, I., Clary, D.C., Crabtree, R.H. and Dannenberg, J.J. (2011) Definition of the Hydrogen Bond (IUPAC Recommendations 2011). *Pure and Applied Chemistry*, **83**, 1637-1641. https://doi.org/10.1351/PAC-REC-10-01-02

[21] Joseph, J. and Jemmis, E.D. (2007) Red-, Blue-, or No-Shift in Hydrogen Bonds: A Unified Explanation. *Journal of the American Chemical Society*, **129**, 4620-4632. https://doi.org/10.1021/ja067545z

[22] Desiraju, G. and Steiner, T. (2001) The Weak Hydrogen Bond: In Structural Chemistry and Biology. Oxford University Press, Oxford, 480. https://doi.org/10.1093/acprof:oso/9780198509707.001.0001

[23] Bondi, A. (1964) Van der Waals Volumes and Radii. *The Journal of Physical Chemistry*, **68**, 441-451. https://doi.org/10.1021/j100785a001

[24] Rowland, R.S. and Taylor, R. (1996) Intermolecular Nonbonded Contact Distances in Organic Crystal Structures: Comparison with Distances Expected from van der

Waals Radii. *The Journal of Physical Chemistry*, **100**, 7384-7391. https://doi.org/10.1021/jp953141+

[25] Cao, Y., Wang, Y., Chen, X. and Ye, J. (2004) Study on Sugar Profile of Rice during Ageing by Capillary Electrophoresis with Electrochemical Detection. *Food Chemistry*, **86**, 131-136. https://doi.org/10.1016/j.foodchem.2003.12.004